Effective Field Theories of Pure and Doped 2-D Quantum Antiferromagnets and High-Precision Tests Based on Quantum Monte Carlo

Uwe-Jens Wiese

Albert Einstein Center for Fundamental Physics
Institute for Theoretical Physics, Bern University

Workshop on
Effective Field Theory for Quantum Many Body Systems
UFT, UAM-CSIC, Madrid, January 16, 2014

Long-term collaborators: Urs Gerber (UNAM Mexico City), Christoph Hofmann (Colima), Fu-Jiun Jiang (NTNU Taipei), Guillermo Palma (Santiago), Nadiia Vlasii (Kiew)

Outline

Outline

Antiferromagnetic precursors of high-T_c superconductors

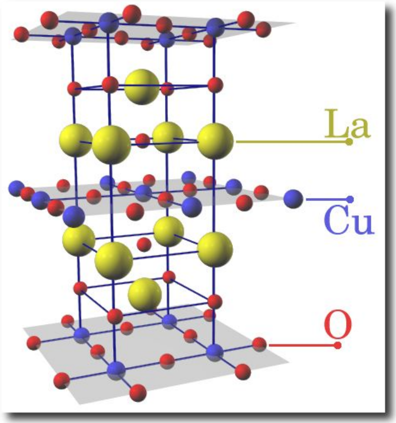

LaCuO

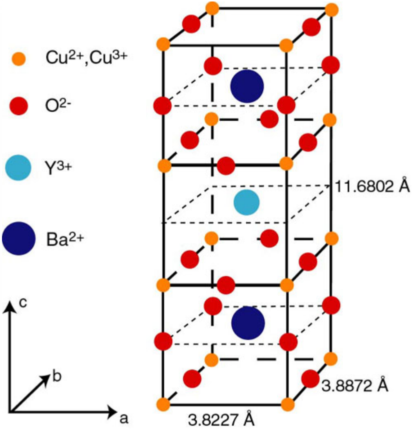

YBaCuO

Properties of cuprates

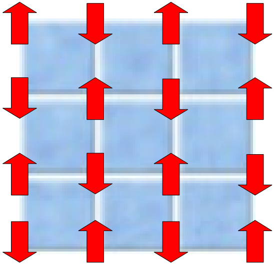

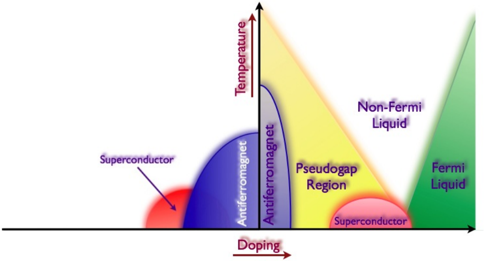

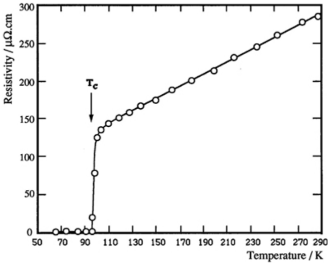

Temperature-dependence of resistivity

Properties of cuprates

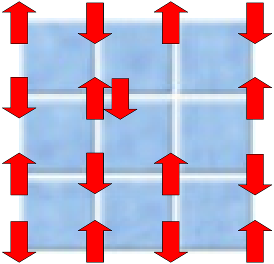

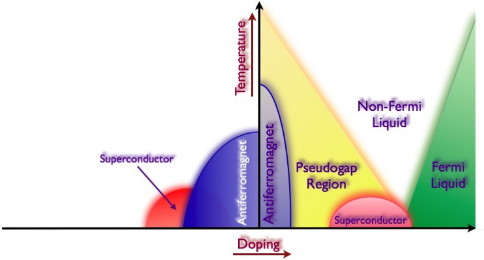

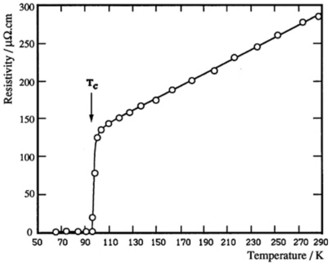

Temperature-dependence of resistivity

Properties of cuprates

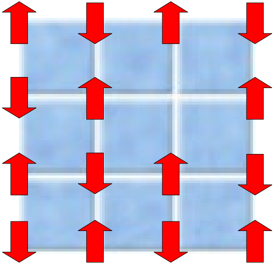

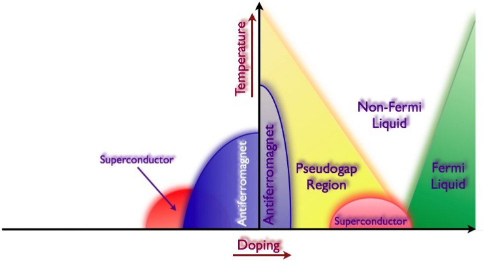

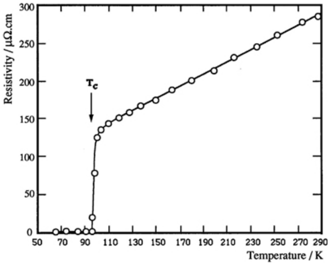

Temperature-dependence of resistivity

Properties of cuprates

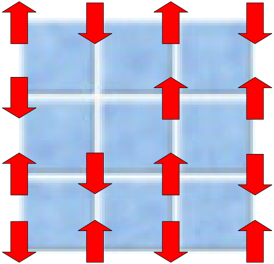

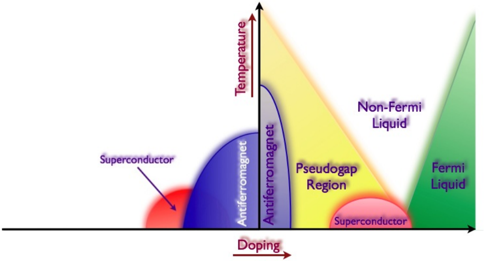

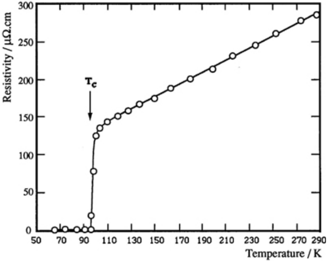

Temperature-dependence of resistivity

Outline

Phase diagrams of QCD and of doped antiferromagnets

QCD phase diagram

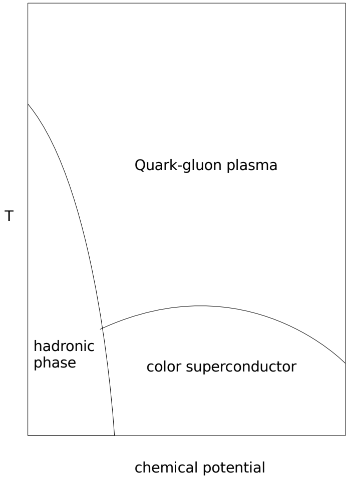

Phase diagram of cuprates

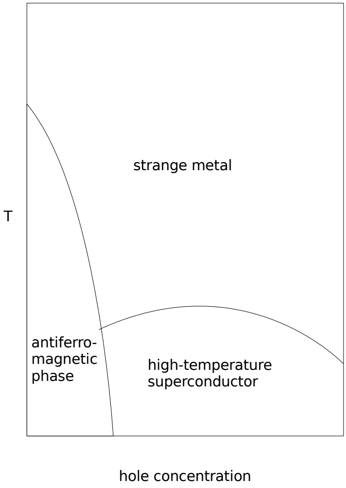

Correspondences between QCD and Antiferromagnetism

	QCD	Antiferromagnetism
broken phase	hadronic vacuum	antiferromagnetic phase
global symmetry	chiral symmetry	spin rotations
symmetry group G	$SU(2)_L \otimes SU(2)_R$	$SU(2)_s$
unbroken subgroup H	$SU(2)_{L=R}$	$U(1)_s$
Goldstone boson	pion	magnon
Goldstone field in G/H	$U(x) \in SU(2)$	$\vec{e}(x) \in S^2$
order parameter	chiral condensate	staggered magnetization
coupling strength	pion decay constant F_π	spin stiffness ρ_s
propagation speed	velocity of light	spin-wave velocity c
conserved charge	baryon number $U(1)_B$	electric charge $U(1)_Q$
charged particle	nucleon or antinucleon	electron or hole
long-range force	pion exchange	magnon exchange
dense phase	nuclear or quark matter	high-T_c superconductor
microscopic description	lattice QCD	Hubbard or t-J model
effective description of Goldstone bosons	chiral perturbation theory	magnon effective theory
effective description of charged fields	baryon chiral perturbation theory	magnon-hole effective theory

Outline

Quantum spins $\vec{S}_x$ on a lattice with sites x

$$[S_x^a, S_y^b] = i\delta_{xy}\varepsilon_{abc}S_x^c, \ \vec{S} = \sum_x \vec{S}_x$$

$SU(2)$ invariant Hamiltonian of the quantum Heisenberg model

$$H = J\sum_{\langle xy\rangle} \vec{S}_x \cdot \vec{S}_y, \ [H, \vec{S}] = 0$$

Partition function at inverse temperature $\beta = 1/T$

$$Z = \mathrm{Tr}\exp(-\beta H)$$

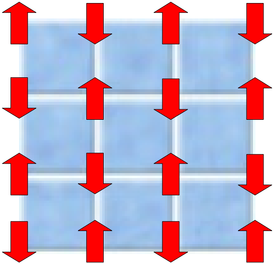

Staggered magnetization order parameter

$$\vec{M}_s = \sum_x (-1)^{(x_1+x_2)/a} \ \vec{S}_x$$

signals spontaneous symmetry breaking $SU(2) \to U(1)$

$$\frac{a^2}{L^2} |\langle \vec{M}_s \rangle| = \mathcal{M}_s \neq 0 \text{ at } T = 0$$

Magnon (Goldstone boson) field in $SU(2)/U(1) = S^2$

$$\vec{e}(x) = (e_1(x), e_2(x), e_3(x)), \quad \vec{e}(x)^2 = 1$$

Low-energy effective action for antiferromagnetic magnons

$$S[\vec{e}] = \int_0^\beta dt \int d^2x \ \frac{\rho_s}{2} \left(\partial_i \vec{e} \cdot \partial_i \vec{e} + \frac{1}{c^2} \partial_t \vec{e} \cdot \partial_t \vec{e} \right)$$

Chakravarty, Halperin, Nelson (1989)
Neuberger, Ziemann (1989)
Hasenfratz, Leutwyler (1990)
Hasenfratz, Niedermayer (1993)
Chubukov, Sentil, Sachdev (1994)

Path integral

$$
\begin{aligned}
Z &= \mathrm{Tr}[\exp(-\varepsilon H_1)\exp(-\varepsilon H_2)\ldots\exp(-\varepsilon H_M)]^N \\
&= \sum_{[s]} \mathrm{Sign}[s]\exp(-S[s])
\end{aligned}
$$

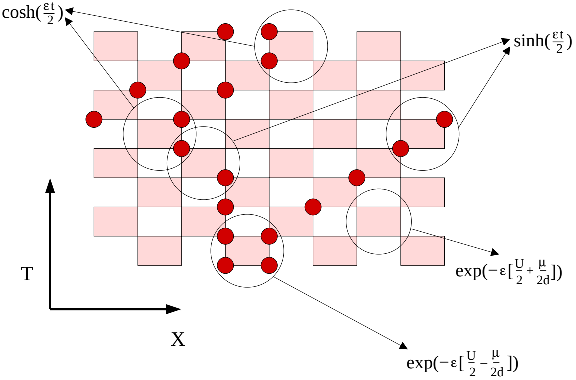

In this case: $M = 2$, $t = U = J$, $\mu = 0$.

Cluster decomposition

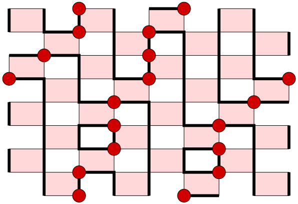

All spins in a cluster are flipped simultaneously with probability $\frac{1}{2}$.

Reference configuration

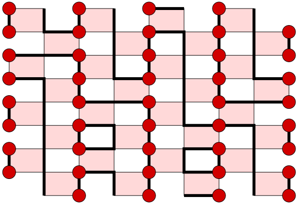

By appropriate cluster flips one can reach the classical Néel state.

Evertz, Lana, Marcu (1993); UJW, Ying (1994); Beard, UJW (1996)

Fit to analytic predictions of effective theory

$$\chi_s = \frac{\mathcal{M}_s^2 L^2 \beta}{3} \left\{ 1 + 2\frac{c}{\rho_s L l}\beta_1(l) + \left(\frac{c}{\rho_s L l}\right)^2 \left[\beta_1(l)^2 + 3\beta_2(l)\right] \right\}$$

$$\chi_u = \frac{2\rho_s}{3c^2} \left\{ 1 + \frac{1}{3}\frac{c}{\rho_s L l}\widetilde{\beta}_1(l) + \frac{1}{3}\left(\frac{c}{\rho_s L l}\right)^2 \left[\widetilde{\beta}_2(l) - \frac{1}{3}\widetilde{\beta}_1(l)^2 - 6\psi(l)\right] \right\}$$

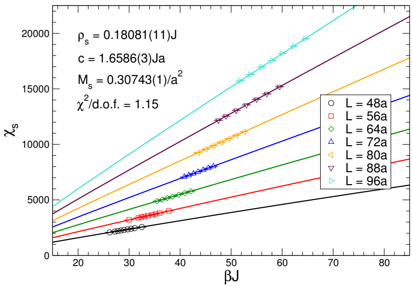

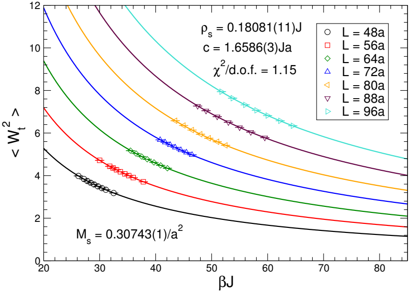

$$\mathcal{M}_s = 0.30743(1)/a^2, \quad \rho_s = 0.18081(11)J, \quad c = 1.6586(3)Ja$$

UJW, Ying (1994); Sandvik, Evertz (2010); Jiang, UJW (2010)

Excellent agreement with effective field theory predictions for the constraint effective potential: Göckeler, Leutwyler (1991)

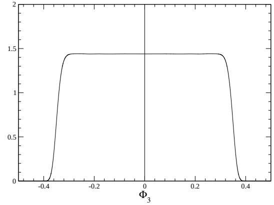

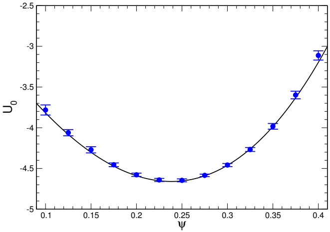

Heisenberg model: Gerber, Hofmann, Jiang, Nyfeler, UJW (2009)
XY model: Gerber, Hofmann, Jiang, Palma, Stebler, UJW (2011)

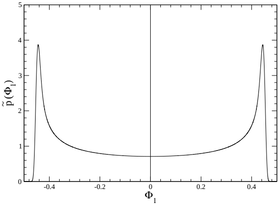

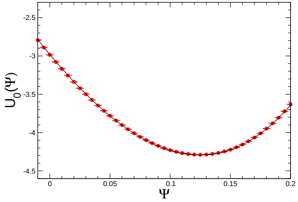

Jiang (2010) $\mathcal{M} = 0.43561(1)/a^2, \ \rho = 0.26974(5)J, \ c = 1.1348(5)Ja$

Effective rotor Lagrange function in the δ-regime $\beta c \gg L$

$$L = \int d^2x \, \frac{\rho_s}{2} \left(\partial_i \vec{e} \cdot \partial_i \vec{e} + \frac{1}{c^2} \partial_t \vec{e} \cdot \partial_t \vec{e} \right) = \frac{\Theta}{2} \partial_t \vec{e} \cdot \partial_t \vec{e}$$

Moment of inertia

$$\Theta = \frac{\rho_s L^2}{c^2} \left[1 + \frac{3.900265}{4\pi} \frac{c}{\rho_s L} + \mathcal{O}\left(\frac{1}{L^2}\right) \right]$$

Hasenfratz, Niedermayer (1993)

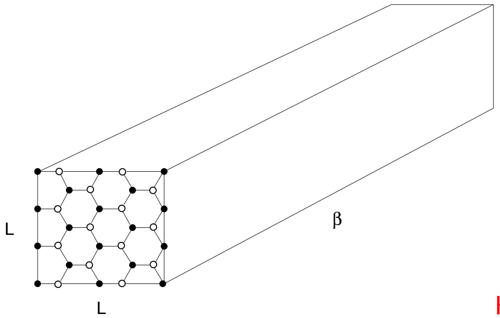

Honeycomb lattice

Jiang (2011): $\widetilde{\mathcal{M}}_s = 0.26885(2), \ \rho_s = 0.1012(1)J, \ c = 1.2900(3)Ja$

Rotor spectrum

$$E_S = \frac{S(S+1)}{2\Theta}$$

Probability distribution of magnetization $M^3 = S^3$

$$p(M^3) = \frac{1}{Z} \sum_{S \geq |M^3|} \exp(-\beta E_S), \quad Z = \sum_{S=0}^{\infty} (2S+1) \exp(-\beta E_S)$$

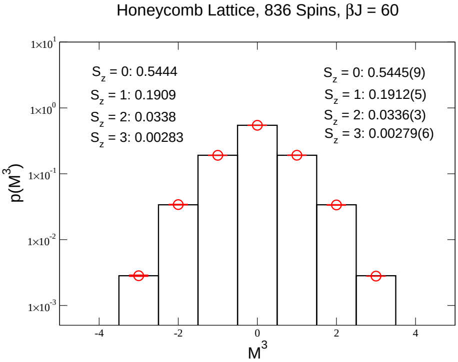

Perfect agreement without any adjustable parameters.

Jiang, Kämpfer, Nyfeler, UJW (2008)

Outline

The Hubbard Model

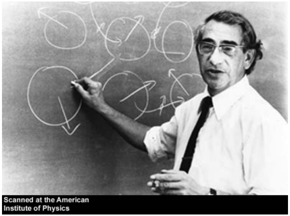

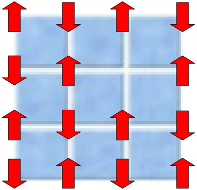

$$H = -t \sum_{\langle xy \rangle} (c_x^\dagger c_y + c_y^\dagger c_x) + U \sum_x (c_x^\dagger c_x - 1)^2, \quad c_x = \begin{pmatrix} c_{x\uparrow} \\ c_{x\downarrow} \end{pmatrix}$$

For large repulsion U it reduces to the t-J model

$$H = P \Big\{ -t \sum_{\langle xy \rangle} (c_x^\dagger c_y + c_y^\dagger c_x) + J \sum_{\langle xy \rangle} \vec{S}_x \cdot \vec{S}_y \Big\} P$$

which further reduces to the Heisenberg model at half-filling

$$H = J \sum_{\langle xy \rangle} \vec{S}_x \cdot \vec{S}_y$$

The Hubbard Model

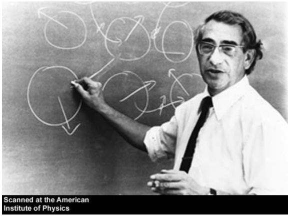

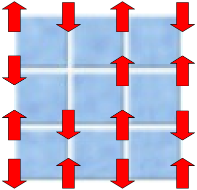

$$H = -t \sum_{\langle xy \rangle} (c_x^\dagger c_y + c_y^\dagger c_x) + U \sum_x (c_x^\dagger c_x - 1)^2, \quad c_x = \begin{pmatrix} c_{x\uparrow} \\ c_{x\downarrow} \end{pmatrix}$$

For large repulsion U it reduces to the t-J model

$$H = P \left\{ -t \sum_{\langle xy \rangle} (c_x^\dagger c_y + c_y^\dagger c_x) + J \sum_{\langle xy \rangle} \vec{S}_x \cdot \vec{S}_y \right\} P$$

which further reduces to the Heisenberg model at half-filling

$$H = J \sum_{\langle xy \rangle} \vec{S}_x \cdot \vec{S}_y$$

Hole dispersion in the t-J model

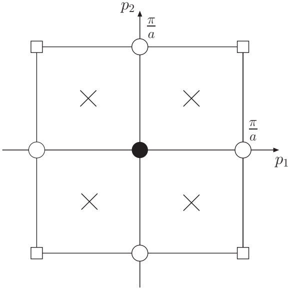

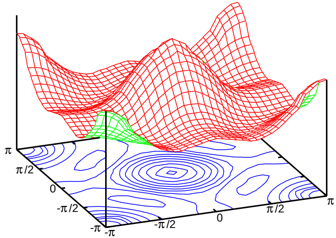

Hole pockets centered at lattice momenta

$$k^{\alpha} = \left(\frac{\pi}{2a}, \frac{\pi}{2a}\right), \quad k^{\alpha\prime} = -k^{\alpha}, \quad k^{\beta} = \left(\frac{\pi}{2a}, -\frac{\pi}{2a}\right), \quad k^{\beta\prime} = -k^{\beta}$$

Hole fields

$$\psi_+^f(x) = \frac{1}{\sqrt{2}}\left[\psi_+^{k^f}(x) - \psi_+^{k^{f\prime}}(x)\right], \quad \psi_-^f(x) = \frac{1}{\sqrt{2}}\left[\psi_-^{k^f}(x) + \psi_-^{k^{f\prime}}(x)\right]$$

Nonlinear realization of the $SU(2)_s$ symmetry

$$u(x)\vec{e}(x)\cdot\vec{\sigma}u(x)^\dagger = \sigma_3, \quad u_{11}(x) \geq 0$$

Under $SU(2)_s$ the diagonalizing field $u(x)$ transforms as

$$u(x)' = h(x)u(x)g^\dagger, \quad u_{11}(x)' \geq 0,$$

$$h(x) = \exp(i\alpha(x)\sigma_3) = \begin{pmatrix} \exp(i\alpha(x)) & 0 \\ 0 & \exp(-i\alpha(x)) \end{pmatrix} \in U(1)_s$$

The composite vector field

$$v_\mu(x) = u(x)\partial_\mu u(x)^\dagger = iv_\mu^a(x)\sigma_a, \quad v_\mu^\pm(x) = v_\mu^1(x) \mp iv_\mu^2(x)$$

transforms as

$$v_\mu^3(x)' = v_\mu^3(x) - \partial_\mu\alpha(x), \quad v_\mu^\pm(x)' = \exp(\pm 2i\alpha(x))v_\mu^\pm(x)$$

Transformation rules of fermion fields

$$
\begin{aligned}
SU(2)_s: &\quad \psi^f_\pm(x)' = \exp(\pm i\alpha(x))\psi^f_\pm(x), \\
U(1)_Q: &\quad {}^Q\psi^f_\pm(x) = \exp(i\omega)\psi^f_\pm(x), \\
D_i: &\quad {}^{D_i}\psi^f_\pm(x) = \mp\exp(ik^f_i a)\exp(\mp i\varphi(x))\psi^f_\mp(x), \\
O: &\quad {}^O\psi^\alpha_\pm(x) = \mp\psi^\beta_\pm(Ox), \quad {}^O\psi^\beta_\pm(x) = \psi^\alpha_\pm(Ox), \\
R: &\quad {}^R\psi^\alpha_\pm(x) = \psi^\beta_\pm(Rx), \qquad {}^R\psi^\beta_\pm(x) = \psi^\alpha_\pm(Rx)
\end{aligned}
$$

Leading terms in the effective Lagrangian for holes

$$
\begin{aligned}
\mathcal{L} \; = \; & \sum_{\substack{f=\alpha,\beta \\ s=+,-}} \Big[M\psi^{f\dagger}_s\psi^f_s + \psi^{f\dagger}_s D_t\psi^f_s + \Lambda\big(\psi^{f\dagger}_s v^s_1\psi^f_{-s} + \sigma_f\psi^{f\dagger}_s v^s_2\psi^f_{-s}\big) \\
+ \; & \frac{1}{2M'} D_i\psi^{f\dagger}_s D_i\psi^f_s + \sigma_f\frac{1}{2M''}\big(D_1\psi^{f\dagger}_s D_2\psi^f_s + D_2\psi^{f\dagger}_s D_1\psi^f_s\big)\Big]
\end{aligned}
$$

Covariant derivative coupling to composite magnon gauge field

$$
D_\mu\psi^f_\pm(x) = \left[\partial_\mu \pm i v^3_\mu(x)\right]\psi^f_\pm(x)
$$

Shraiman, Siggia (1988); Wen (1989); Shankar (1989); Sushkov (1994); Brügger, Kämpfer, Moser, Pepe, UJW (2006)

Outline

Magnon exchange

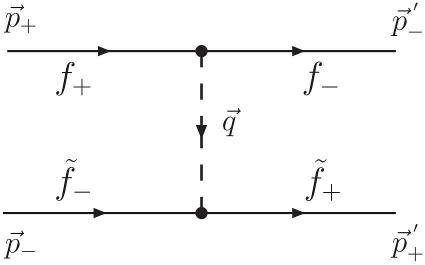

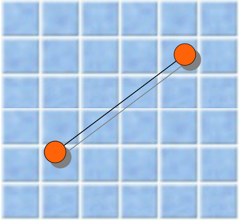

One-magnon exchange potentials

$$V^{\alpha\alpha}(\vec{r}) = \gamma \frac{\sin(2\varphi)}{r^2}, \quad V^{\beta\beta}(\vec{r}) = -\gamma \frac{\sin(2\varphi)}{r^2},$$

$$V^{\alpha\beta}(\vec{r}) = V^{\beta\alpha}(\vec{r}) = \gamma \frac{\cos(2\varphi)}{r^2}, \quad \gamma = \frac{\Lambda^2}{2\pi\rho_s}$$

Two-hole Schrödinger equation for an $\alpha\beta$ pair

$$\begin{pmatrix} -\frac{1}{M'}\Delta & V^{\alpha\beta}(\vec{r}) \\ V^{\alpha\beta}(\vec{r}) & -\frac{1}{M'}\Delta \end{pmatrix} \begin{pmatrix} \Psi_1(\vec{r}) \\ \Psi_2(\vec{r}) \end{pmatrix} = E \begin{pmatrix} \Psi_1(\vec{r}) \\ \Psi_2(\vec{r}) \end{pmatrix}$$

Making the ansatz

$$\Psi_1(\vec{r}) \pm \Psi_2(\vec{r}) = R(r)\chi_\pm(\varphi)$$

for the angular part of the wave function one obtains

$$-\frac{d^2\chi_\pm(\varphi)}{d\varphi^2} \pm M'\gamma\cos(2\varphi)\chi_\pm(\varphi) = -\lambda\chi_\pm(\varphi)$$

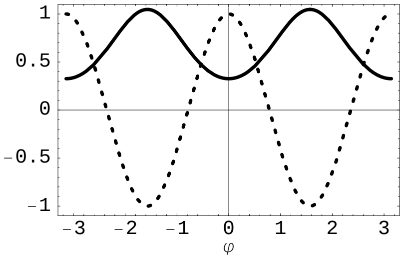

looks like s-wave,
but turns out to be p-wave

Two-hole bound states of $\alpha\beta$ and $\alpha\alpha$ pairs

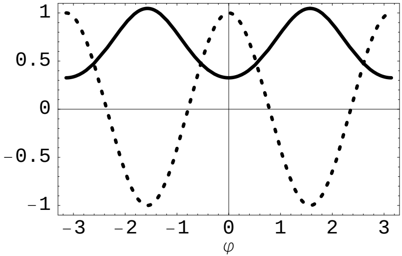

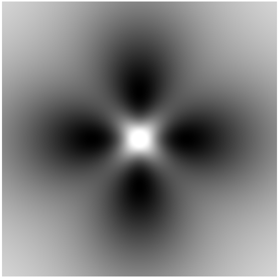

Angular wave function

Probability density

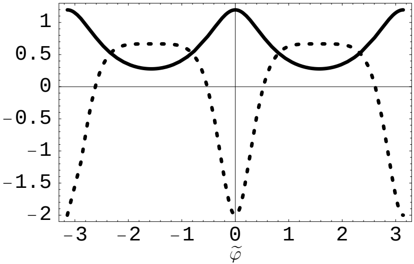

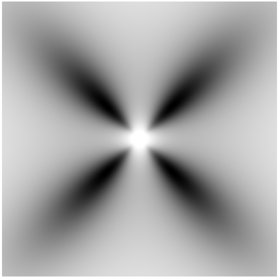

Outline

Topologically conserved current

$$j_\mu(x) = \frac{1}{8\pi}\varepsilon_{\mu\nu\rho}\vec{e}(x)\cdot[\partial_\nu\vec{e}(x)\times\partial_\rho\vec{e}(x)]\,,\ \partial_\mu j_\mu(x) = 0$$

Topological winding number

$$n[\vec{e}] = \int d^2x\ j_t = \frac{1}{8\pi}\int d^2x\ \varepsilon_{ij}\vec{e}\cdot[\partial_i\vec{e}\times\partial_j\vec{e}] \in \Pi_2[S^2] = \mathbb{Z},$$

Schwarz inequality for the energy

$$E[\vec{e}] = \int d^2x\ \frac{\rho_s}{2}\partial_i\vec{e}\cdot\partial_i\vec{e} \geq 4\pi\rho_s|n[\vec{e}]|$$

Selfduality condition

$$\partial_i\vec{e} + \varepsilon_{ij}\partial_j\vec{e}\times\vec{e} = 0$$

is satisfied by Skyrmion configurations

$$\vec{e}_{\rho,\gamma}(r,\chi) = \left(\frac{2r\rho}{r^2+\rho^2}\cos(\chi+\gamma), \frac{2r\rho}{r^2+\rho^2}\sin(\chi+\gamma), \frac{r^2-\rho^2}{r^2+\rho^2}\right)$$

Single-Hole-Skyrmion Hamiltonian

$$
\begin{aligned}
H^f \Psi^f(r,\chi,\gamma) &= \begin{pmatrix} H^f_{++} & H^f_{+-} \\ H^f_{-+} & H^f_{--} \end{pmatrix} \begin{pmatrix} \Psi^f_+(x) \\ \Psi^f_-(x) \end{pmatrix} = E^f \Psi^f(x), \\
H^f_{++,--} &= -\frac{1}{2M'}\left[\partial_r^2 + \frac{1}{r}\partial_r - \frac{1}{r^2}\left(-i\partial_\chi \pm \frac{\rho^2}{r^2+\rho^2}\right)^2\right] \\
&+ \frac{1}{2\mathcal{I}(\rho)}\left(-i\partial_\gamma \mp \frac{\rho^2}{r^2+\rho^2}\right)^2, \\
{H^f_{+-}}^* &= H^f_{-+} = \sqrt{2}\Lambda\sigma_f \frac{\rho}{r^2+\rho^2} \exp\left(i\left[2\chi + \gamma + \sigma_f \frac{\pi}{4}\right]\right)
\end{aligned}
$$

Single-hole-Skyrmion wave function

$$
\Psi^f_{m_+,m_-,m}(r,\chi,\gamma) = \\
\begin{pmatrix} \psi_+(r)\exp\left(i\left[m_+\chi - \sigma_f \frac{\pi}{8}\right]\right)\exp(i(m-\frac{1}{2})\gamma) \\ \sigma_f\psi_-(r)\exp\left(i\left[m_-\chi + \sigma_f \frac{\pi}{8}\right]\right)\exp(i(m+\frac{1}{2})\gamma) \end{pmatrix}
$$

Two hole-Skyrmion wave function

$$\Psi^{\alpha\beta}_{m_+^\alpha,,m_-^\alpha,m_+^\beta,m_-^\beta,m}(r_\alpha,\chi_\alpha,r_\beta,\chi_\beta,\gamma) =$$

$$\begin{pmatrix} \psi_{++}(r_\alpha,r_\beta)\exp\left(i\left[m_+^\alpha\chi_\alpha + m_+^\beta\chi_\beta\right]\right)\exp(i(m-1)\gamma) \\ -\psi_{+-}(r_\alpha,r_\beta)\exp\left(i\left[m_+^\alpha\chi_\alpha + m_-^\beta\chi_\beta - \frac{\pi}{4}\right]\right)\exp(im\gamma) \\ \psi_{-+}(r_\alpha,r_\beta)\exp\left(i\left[m_-^\alpha\chi_\alpha + m_+^\beta\chi_\beta + \frac{\pi}{4}\right]\right)\exp(im\gamma) \\ -\psi_{--}(r_\alpha,r_\beta)\exp\left(i\left[m_-^\alpha\chi_\alpha + m_-^\beta\chi_\beta\right]\right)\exp(i(m+1)\gamma) \end{pmatrix}$$

90 degrees rotation of two-hole-Skyrmion ground state

$$^O\Psi^{\alpha\beta}_{-1,1,-1,1,0}(r_\alpha,\chi_\alpha,r_\beta,\chi_\beta,\gamma) = -i\Psi^{\alpha\beta}_{-1,1,-1,1,0}(r_\alpha,\chi_\alpha,r_\beta,\chi_\beta,\gamma)$$

The bound state of two holes localized on a Skyrmion again has p-wave symmetry and is thus not a candidate for a preformed Cooper pair in a high-temperature superconductor.

Vlasii, Jiang, Hofmann, UJW (2012)

Outline

Hubbard model on the honeycomb lattice: Unbroken $SU(2)_s$ symmetric phase (graphene)

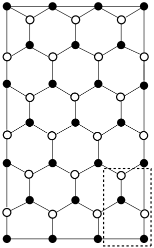

Honeycomb lattice

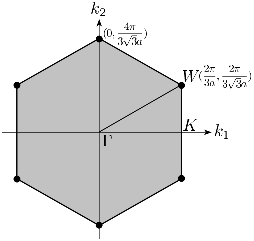

Brillouin zone

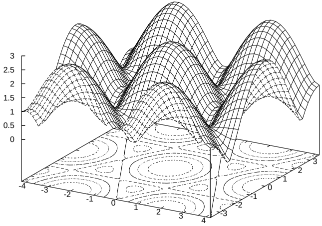

Dispersion relation

Effective Dirac Lagrangian for free graphene

$$\mathcal{L} = \sum_{\substack{f=\alpha,\beta \\ s=+,-}} \overline{\psi}_s^f \gamma_\mu \partial_\mu \psi_s^f$$

Hole dispersion in the t-J model ($Na_xCoO_2 \cdot yH_2O$)

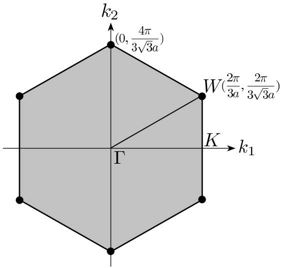

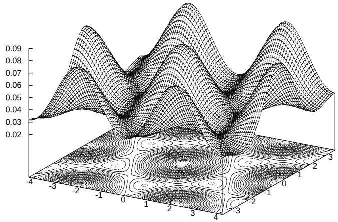

Effective Lagrangian for Magnons and Holes

$$\mathcal{L} = \sum_{\substack{f=\alpha,\beta \\ s=+,-}} \Big[M\psi_s^{f\dagger}\psi_s^f + \psi_s^{f\dagger} D_t \psi_s^f + \frac{1}{2M'} D_i \psi_s^{f\dagger} D_i \psi_s^f$$

$$+ \Lambda \psi_s^{f\dagger}(isv_1^s - \sigma_f v_2^s)\psi_{-s}^f \Big] + \frac{\rho_s}{2}\left(\partial_i \vec{e} \cdot \partial_i \vec{e} + \frac{1}{c^2}\partial_t \vec{e} \cdot \partial_t \vec{e}\right)$$

Hofmann, Jiang, Kämpfer, Nyfeler, UJW (2008)

Conclusions

• Doped antiferromagnets are described quantitatively by systematic low-energy effective field theories for magnons and doped holes.

• Quantum Monte Carlo calculations using the loop-cluster algorithm yield the low-energy parameters with fraction of a per mille accuracy.

• After fixing the low-energy parameters, the Monte Carlo data provide a very high-accuracy quantitative test of the magnon effective theory.

• Through the Shraiman-Siggia coupling, magnon exchange binds hole pairs in the p-wave channel.

• Two holes localized on a Skyrmion again have p-wave symmetry. Only if binding also exists in the d-wave channel, such states may be a candidate for a preformed Cooper pair in a high-T_c superconductor.

• Systems on the honeycomb lattice as well as electron-doped systems have been investigated with the same techniques.

• On the honeycomb lattice, two holes bound by magnon exchange have f-wave symmetry.